J. Fluid Mech. (2015), *vol.* 766, R2, doi:10.1017/jfm.2015.38

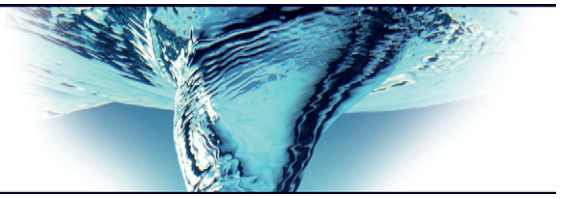

JFM RAPIDS
journals.cambridge.org/rapids

Orientation and rotation of inertial disk particles in wall turbulence

Niranjan Reddy Challabotla[1], Lihao Zhao[1,†] and Helge I. Andersson[1]

[1]Department of Energy and Process Engineering, Norwegian University of Science and Technology, 7491 Trondheim, Norway

(Received 20 November 2014; revised 9 January 2015; accepted 16 January 2015; first published online 9 February 2015)

The translational and rotational dynamics of oblate spheroidal particles suspended in a directly simulated turbulent channel flow have been examined. Inertial disk-like particles exhibited a significant preferential orientation in the plane of the mean shear. The rotational inertia about the symmetry axis of the disk-like particles hampered the spin-up of the flattest particles to match the mean flow vorticity. The influence of the particle shape on the orientation and rotation diminished as the translational inertia increased from Stokes number 1 to 30. An isotropization of both orientation and rotation could be observed in the core region of the channel. The translational motion of the oblate spheroids had a weak dependence on the aspect ratio. We therefore concluded that inertial particles sample nearly the same flow field irrespective of shape. Nevertheless, the orientation and rotation of disk-like particles turned out to be qualitatively different from the dynamics of fibre-like particles.

Key words: multiphase and particle-laden flows, particle/fluid flows, turbulent flows

1. Introduction

The dynamics of non-spherical particles is commonly investigated by assuming regular axisymmetric shapes, i.e. either prolate (rod-like) or oblate (disk-like) spheroids. The vast majority of studies have focused on rod-like particles due to their relevance in paper making, polymer processing, biomass combustion and dispersion of micro-organisms and aerosols. In contrast, investigations of the dynamics of disk-like particles are scarce. Disk-like particles occur as air pollutants, natural clay minerals and blood constituents, in drug delivery applications (Kleinstreuer & Feng 2013) and ice crystal formation in clouds (Siewert *et al.* 2014) and as flakes used for flow visualizations (Gauthier, Gondret & Rabaud 1998).

Investigations of the dynamics of an individual spheroidal particle in a laminar-like flow can be considered as a starting point for studies of spheroid suspensions in

† Email address for correspondence: lihao.zhao@ntnu.no

turbulence. The rotational dynamics of a single spheroidal particle in creeping flow has been subjected to extensive theoretical studies (Jeffery 1922; Brenner 1964; Harper & Chang 1968). A series of theoretical and experimental investigations were conducted to understand the orderly nature of non-spherical particle motion in laminar flows (Gallily & Cohen 1979). The importance of particle inertia on the dynamics of spheroidal particles was assessed by numerical integrations of the equations governing the particle dynamics by Lundell & Carlsson (2010) for prolate spheroids and by Challabotla, Nilsen & Andersson (2015) for oblate spheroids. A comprehensive review of computational analyses of non-spherical particle transport and its application in lung aerosol dynamics was provided by Kleinstreuer & Feng (2013).

Methodologies developed for a single spheroidal particle have been adopted to investigate dilute suspensions of spheroidal particles in turbulent flows. Fan & Ahmadi (1995) developed a methodology to investigate the dispersion and deposition of spheroidal particles in an isotropic pseudo-turbulent flow field, and their methodology was subsequently extended by Zhang *et al.* (2001) to investigate spheroidal particle transport and deposition in fully developed turbulent channel flow using direct numerical simulation (DNS). Mortensen *et al.* (2008*a*,*b*), Marchioli, Fantoni & Soldati (2010) and Marchioli & Soldati (2013) studied the dynamics of a wide range of prolate (rod-like) spheroidal particle suspensions in turbulent channel flow using DNS and reported detailed statistics for translational, orientational and rotational motions. A brief review of the modelling of anisotropic particles in a turbulent flow environment was reported by Andersson & Soldati (2013).

Only a few studies have focused on suspensions of oblate (disk-like) spheroids in turbulent flows. Knowledge about the dynamics of disk-like particles is therefore far less complete than for their rod-like counterparts. Klett (1995) carried out a theoretical investigation to develop orientational models for various shapes of non-spherical particles in turbulent flows. Parsa *et al.* (2012) reported results from a computational study of rotation rates of anisotropic tracer particles in homogeneous isotropic turbulence. The orientation of the non-spherical tracers correlated with the fluid velocity gradient tensor and the particles preferentially sampled the flow field. The mean-square rotation rate of disk-like particles turned out to be much closer to being randomly oriented than for fibre-like particles. Later, these results were experimentally confirmed by Marcus *et al.* (2014). Tumbling of small inertial non-spherical particles in random and turbulent flows was investigated by Gustavsson, Einarsson & Mehlig (2014). Njobuenwu & Fairweather (2014) investigated the dynamics of both prolate and oblate spheroids by means of large-eddy simulations and concluded that the shape of the particle is an important factor when designing and optimizing industrial processes. Siewert *et al.* (2014) reported orientational statistics for various types of ellipsoidal particles embedded in a DNS of isotropic decaying turbulence. Particle-resolved simulations using an immersed boundary method for finite-sized spherical particles (Uhlmann 2008; Lucci, Ferrante & Elghobashi 2010) and a lattice Boltzmann method for spheroidal particles (Do-Quang *et al.* 2014) have recently emerged. At present these computationally expensive approaches are unable to handle suspensions of millions of small finite size particles, as often required to obtain reliable particle statistics in a turbulent flow environment. To the best of the authors' knowledge, DNS of oblate spheroids suspended in a turbulent channel flow has never been performed.

The goal of the present study is to complement the existing DNS studies of turbulent suspensions of inertial fibre-like prolate spheroids with data from simulations of disk-like oblate spheroids embedded in wall turbulence. It is anticipated that

disk-like particles will orient themselves and rotate rather differently from fibre-like particles. We also anticipate that inertial disks will exhibit a fundamentally different response to a turbulent flow field than the inertia-free tracers studied by Parsa *et al.* (2012). Our aim is accordingly to assess the effect of the particle shape, parameterized by the aspect ratio, in combination with the particle mass, parameterized by a Stokes number based on translational inertia, on the orientation of disk-like particles and the resulting translational and rotational dynamics. In the interpretation of the results, it is essential to distinguish between the influence of translational and rotational inertia.

2. Methodology

The dynamics of rigid disk-like particles suspended in channel flow turbulence is modelled in an Eulerian–Lagrangian approach. The continuous Newtonian fluid phase, in which the disks are suspended, is governed by continuity and Navier–Stokes equations.

A general spheroidal particle is characterized by three semiaxes $a = b \neq c$. The aspect ratio $\lambda = c/a$ distinguishes between prolate ($\lambda > 1$) and oblate ($\lambda < 1$) spheroids, whereas $\lambda = 1$ corresponds to an isotropic particle, i.e. a sphere. Prolate spheroidal point particles suspended in a turbulent channel flow were first studied by Zhang *et al.* (2001), followed by Mortensen *et al.* (2008*a*,*b*), Marchioli *et al.* (2010) and Marchioli & Soldati (2013). Here, the same methodology is adopted to study the dynamics of oblate spheroidal point particles in channel flow turbulence. The translational and rotational motions of one single spheroidal particle obey

$$m\frac{\mathrm{d}v_i}{\mathrm{d}t} = F_i, \quad I'_{ij}\frac{\mathrm{d}\omega'_j}{\mathrm{d}t} + \epsilon_{ijk}\omega'_j I'_{kl}\omega'_l = N'_i, \tag{2.1a,b}$$

where ϵ_{ijk} is the Levi-Civita alternating or permutation tensor. Two different Cartesian frames of reference are used. The translational motion of a disk-like spheroid is governed by Newton's second law of motion (2.1*a*), expressed in the inertial reference frame $x_i = \langle x_1, x_2, x_3\rangle$, in which the turbulent flow field is obtained. The rotational motion is governed by Euler's equation (2.1*b*), which is formulated in a particle frame $x'_i = \langle x'_1, x'_2, x'_3\rangle$ with its origin in the mass centre and the coordinate axes aligned with the principal directions of inertia of the spheroid. Thus, $v_i = \mathrm{d}x_i/\mathrm{d}t$ denotes the translational particle velocity in the inertial frame, whereas ω'_i is the angular velocity of the spheroid in the particle frame and I'_{ij} is the moment of inertia tensor. To focus on the crucial effects of particle aspect ratio and inertia, the gravity and lift forces are ignored in the present study. The disk-like spheroids are sufficiently small to justify the point-particle approach and the particle Reynolds number Re_p based on the major axis of the disk and the mean slip velocity is everywhere smaller than unity. Under these conditions the neighbouring flow can be considered as Stokesian and the drag force F_i acting on a spheroid from the surrounding fluid can be expressed as

$$F_i = \mu K_{ij}(u_j - v_j), \tag{2.2}$$

where u_j is the fluid velocity at the particle location in the x_j direction. Here, the resistance tensor K_{ij} is represented in the inertial frame and related to the resistance tensor K'_{ij} in the particle frame as $K_{ij} = A^t_{ik}K'_{kl}A_{lj}$, where A_{ij} denotes the orthogonal transformation matrix which relates the same vector in the two different frames through the linear transformation $x_i = A_{ij}x'_j$. The right-hand side of (2.2) represents

the hydrodynamic drag force acting on a spheroidal particle, as derived by Brenner (1964). The resistance tensor K'_{ij} is a diagonal matrix with elements

$$\left.\begin{aligned} K'_{xx} = K'_{yy} &= \frac{32\pi a(1-\lambda^2)^{3/2}}{(3-2\lambda^2)(\pi - C) - 2\lambda(1-\lambda^2)^{1/2}}, \\ K'_{zz} &= \frac{16\pi a(1-\lambda^2)^{3/2}}{(1-2\lambda^2)(\pi - C) + 2\lambda(1-\lambda^2)^{1/2}}, \end{aligned}\right\} \tag{2.3}$$

where $C = 2\tan^{-1}(\lambda(1-\lambda^2)^{-1/2})$ and x'_3 (or z') is the symmetry axis of the spheroid.

The torque components N'_i for a three-axial ellipsoidal particle in creeping shear flow originally derived by Jeffery (1922) simplify for a spheroid to

$$\left.\begin{aligned} N'_1 &= \frac{16\pi\mu a^3\lambda}{3(\beta_0 + \lambda^2\gamma_0)}[(1-\lambda^2)S'_{23} + (1+\lambda^2)(\Omega'_1 - \omega'_1)], \\ N'_2 &= \frac{16\pi\mu a^3\lambda}{3(\alpha_0 + \lambda^2\gamma_0)}[(\lambda^2-1)S'_{13} + (1+\lambda^2)(\Omega'_2 - \omega'_2)], \\ N'_3 &= \frac{32\pi\mu a^3\lambda}{3(\alpha_0 + \beta_0)}(\Omega'_3 - \omega'_3). \end{aligned}\right\} \tag{2.4}$$

Here, S'_{ij} and Ω'_i denote the fluid rate-of-strain tensor and rate-of-rotation vector respectively. These expressions are valid for any aspect ratio λ as long as the shape factors α_0, β_0 and γ_0 are defined as semi-infinite integrals. However, the analytical expressions for the shape factors for oblate spheroids due to Siewert *et al.* (2014),

$$\left.\begin{aligned} \alpha_0 = \beta_0 &= -\frac{\lambda}{2(1-\lambda^2)^{3/2}}[C - \pi + 2\lambda(1-\lambda^2)^{1/2}], \\ \gamma_0 &= \frac{1}{(1-\lambda^2)^{3/2}}[\lambda C - \lambda\pi + 2(1-\lambda^2)^{1/2}], \end{aligned}\right\} \tag{2.5}$$

are different from the shape factors derived by Gallily & Cohen (1979) for prolate spheroids. We have already used the above expressions to deduce the explicit expressions (2.3) for the non-zero elements of the resistance tensor. These expressions for K'_{ij} are also applicable only for oblate spheroids and differ from those derived by Gallily & Cohen (1979) for prolate spheroids and subsequently used by Zhang *et al.* (2001) and Mortensen *et al.* (2008*a*,*b*) for elongated spheroids.

The ability of an inertial particle to adjust to the ambient flow field can be estimated in terms of a particle response time τ_p. Shapiro & Goldenberg (1993) introduced a translational relaxation time based on the orientation-averaged resistance tensor $\bar{K} = 3(K'^{-1}_{xx} + K'^{-1}_{yy} + K'^{-1}_{zz})^{-1}$. This is believed to be a relevant time scale for isotropically oriented particles and has been used by Mortensen *et al.* (2008*a*) and others in their studies of prolate spheroids. We now adopt the same definition of an equivalent response time for the oblate spheroids. By means of the elements of the translational resistance tensor in (2.3) valid only for $\lambda < 1$, we obtain

$$\tau_p \equiv \frac{4D\pi a^3}{3\nu}\frac{\lambda}{\bar{K}} = \frac{2Da^2}{9\nu}\frac{\lambda(\pi - C)}{2(1-\lambda^2)^{1/2}}, \tag{2.6}$$

where D is the ratio between the particle and fluid densities. A Stokes number St is then defined as the ratio between τ_p and the viscous time scale $\tau_v = \nu/u_\tau^2$ based on the wall-friction velocity u_τ and thus representative of the near-wall turbulence.

We use DNS to simulate a turbulent channel flow at Reynolds number $Re_\tau = 180$ based on u_τ and the channel half-height h. The computational set-up and the flow solver are essentially the same as in the preceding simulation studies of dilute suspensions of elongated spheroids in turbulent channel flow reported by Mortensen *et al.* (2008*a*,*b*) and Zhao, Marchioli & Andersson (2014). In the present work it is also assumed that the particle suspension is sufficiently dilute that one-way coupled simulations can be justified and particle–particle collisions are rare and therefore neglected. Particle–wall collisions are fully elastic so that a spheroid keeps its linear momentum in the two homogenous directions as well as its angular momentum upon touching the wall. A collision is defined to occur every time that the distance from the centre of mass of a disk to the closest wall becomes less than the semimajor axis a. The size of the disks does not exceed the Kolmogorov length scale. The assumption of Stokes flow in the immediate vicinity of a particle, on which the expressions for the force and torque components in (2.2) and (2.4) are based, can thus be justified.

Ten simulations are performed for oblate spheroids with aspect ratios of $\lambda = 0.01$, 0.1, 0.33, 0.5 and 1, all for both Stokes numbers, $St = 1$ and 30. The actual simulation is performed with $\lambda = 0.999$ rather than $\lambda = 1$ (for which a singularity arises) and compared with data from a tailor-made version of the code for spherical particles. For each of the ten particle parameter combinations, 500 000 oblate spheroids with semimajor axis $a^+ = 0.36$ are injected randomly into the same turbulence field. The Stokes number is varied for a given aspect ratio by altering the density ratio D. Orientational and rotational particle statistics are computed by averaging instantaneous data in time between $5400\tau_v$ and $10\,800\tau_v$ and also in the homogeneous streamwise and spanwise directions.

3. Results and discussion

The particle shape, parameterized by the aspect ratio λ, turned out to have only a minor influence on the translational motion of the oblate spheroids, especially for the most inertial particles. The mean velocity and the r.m.s. of the velocity fluctuations closely resembled earlier results reported for spherical particles (Marchioli *et al.* 2008) and for prolate spheroids (Mortensen *et al.* 2008*a*,*b*; Zhao *et al.* 2014). Zhao *et al.* (2014) observed that the aspect ratio effect for fibre-like particles vanished at high Stokes numbers and concluded that the translational motion is controlled only by inertia through preferential concentration. The modest shape effect on the translational motion statistics observed also for the oblate spheroids suggests that these disk-like particles sample nearly the same flow regions as spherical and fibre-like particles. Nevertheless, the particle aspect ratio λ turns out to have a major influence on the orientational and rotational statistics, as the present results will demonstrate. The distribution, orientation and rotation of oblate spheroids with $\lambda = 0.33$ are shown in the snapshots in figure 1. Although the disk-like particles are injected uniformly into the turbulent flow field, they tend to accumulate in the near-wall region, and this tendency is strongest for the particles with the highest inertia in figure 1(*b*). The particles are furthermore seen to rotate faster in the near-wall region than in the core region of the channel. This suggests that the particles tend to spin up trying to adapt to the locally high fluid rotation, i.e. half of the mean vorticity $\mathrm{d}U^+/\mathrm{d}z^+$. The circular shape of the projections of the majority of the particles into the (x, z) plane in the near-wall region reveals that the disk-like particles exhibit a strong preferential orientation, with the symmetry axis aligned with the mean vorticity vector. On the contrary, the particles

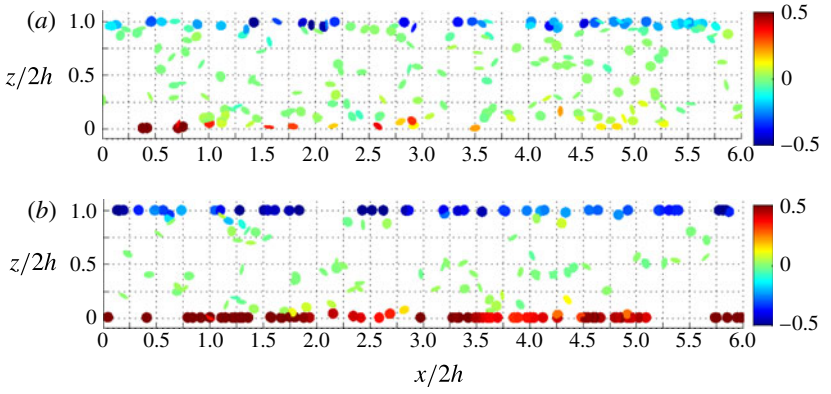

FIGURE 1. Instantaneous distribution of disk-like particles with aspect ratio $\lambda = 0.33$ projected into the (x, z) plane. The shape reflects the particle orientation and the colour coding refers to the particle spanwise angular velocity ω_y normalized by the viscous time scale τ_v: (*a*) $St = 1$; (*b*) $St = 30$.

seem to be randomly oriented in the core region where the vorticity field is almost isotropic. The preferential orientation of the oblate spheroids observed in figure 1 is qualitatively different from that of prolate spheroids reported by Mortensen *et al.* (2008*a*,*b*) and Marchioli *et al.* (2010). They found a preferential alignment in the streamwise direction in the near-wall region. This preferential orientation was most pronounced for high aspect ratios ($\lambda \gg 1$) and modest inertia, contrary to figure 1 which shows that the preferential orientation of the disk-like particles with $\lambda = 0.33$ increases with inertia. The qualitative trends seen in the snapshots in figure 1 are now to be quantified by means of orientational and rotational particle statistics.

Figure 2 shows the variations of the mean of the absolute values of the particle direction cosines from the wall at $z^+ = 0$ to the channel centre at $z^+ = 180$. A direction cosine $|\cos\theta_i|$ is defined in terms of the angle θ_i between the symmetry axis of an oblate spheroid and the x_i-direction of the inertial reference frame. The results for the high-Stokes-number particles show a strong preferential orientation in the spanwise y-direction near the channel walls, i.e. $|\cos\theta_y| \approx 1$. This is consistent with our recent finding that a single inertial disk-like particle in uniform shear flow ultimately tends to rotate in the flow-gradient plane (Challabotla *et al.* 2015). The flattest disks ($\lambda = 0.01$) with modest inertia ($St = 1$), however, exhibit a strong preferential orientation in the wall-normal z-direction in the vicinity of the walls ($z^+ \lesssim 50$), i.e. $|\cos\theta_z| \approx 1$. This tendency is shape-dependent since the inertia effect is modest for $St = 1$ and most pronounced for the flattest spheroids. This is consistent with results reported by Gustavsson *et al.* (2014), namely that an inertia-free disk aligns the symmetry axis preferentially orthogonal to the vorticity vector in homogeneous isotropic turbulence. With increasing inertia, i.e. higher Stokes number, the preferential orientation is in the spanwise rather than in the wall-normal direction, so that the symmetry axis becomes aligned with the mean vorticity. This change of the preferred disk orientation occurs when inertia becomes more influential than shape. The trends observed herein are at variance with those observed for fibre-like particles by Mortensen *et al.* (2008*a*,*b*) and Marchioli *et al.* (2010). However, a common feature of disk-like and fibre-like particles is that both tend to align their major axis in the streamwise direction.

In the central region of the channel, however, all three mean direction cosines $|\cos\theta_i|$ approach 0.5 and accordingly reflect an isotropic orientation. This isotropization

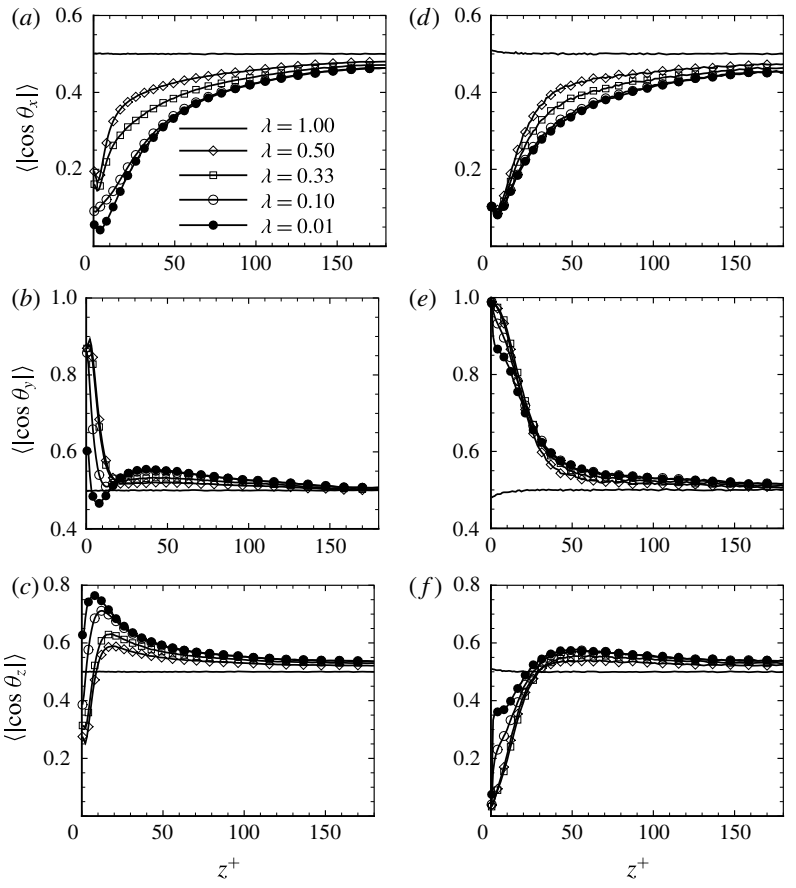

FIGURE 2. The mean absolute values $\langle|\cos\theta_i|\rangle$ of direction cosines: (*a–c*) $St = 1$; (*d–f*) $St = 30$.

is obviously a consequence of the almost isotropic turbulence field in the channel core. No mechanisms exist to enforce orientational anisotropies and all spheroids irrespective of their inertia (St) and shape (λ) orient randomly. For the same reason a receding influence of inertia and shape was found for fibre-like particles by Mortensen *et al.* (2008*a*,*b*).

The rotation of a non-spherical particle is obviously affected by the particle orientation. The spanwise component $\langle\omega_y\rangle$ of the mean angular velocity or spin vector is presented in figure 3, whereas the two other mean spin components are zero in the present flow configuration. The spanwise spin $\langle\omega_y\rangle$ of a spherical particle ($\lambda = 1$) increases monotonically from the centre region towards the channel walls and approaches 0.5, i.e. matches the mean angular velocity $\langle\Omega_y\rangle = 0.5\mathrm{d}U^+/\mathrm{d}z^+$ of the fluid. For $St = 1$, the flattest disks ($\lambda = 0.01$) rotate substantially slower than the spheres next to the wall. This strong shape effect in figure 3 can be attributed to the distinct aspect ratio effect on the preferential orientation of $St = 1$ particles, as shown in figure 2. One may conjecture that the flattest disks are mostly in Jeffery-like orbits with their symmetry axis almost perpendicular to the wall and they rarely tumble. This explains the modest $\langle\omega_y\rangle$ seen in figure 3(*a*). The alignment with the mean fluid vorticity vector increases with λ, and so does the mean spin $\langle\omega_y\rangle$. Likewise, the more

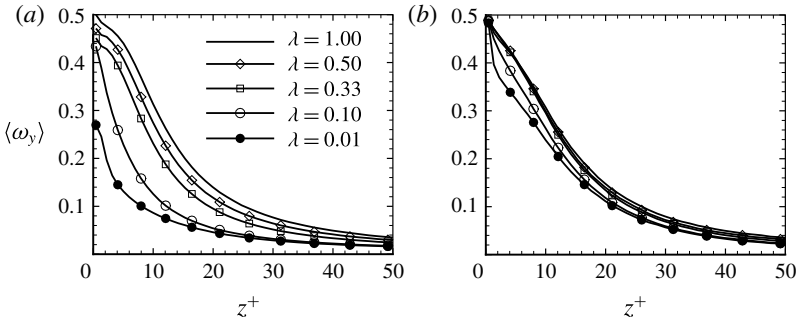

FIGURE 3. Mean spanwise angular velocity $\langle\omega_y\rangle$ normalized by the viscous time scale τ_v: (*a*) $St = 1$; (*b*) $St = 30$.

inertial particles in figure 3(*b*) rotate faster than those in figure 3(*a*). This is consistent with the stronger preferential orientation seen in figure 2 which enables the disk-like particles to be spun up almost to the fluid spin $\langle\Omega_y\rangle$. Since the preferential orientation of the Stokes number 30 particles is only weakly dependent on the particle aspect ratio, so are the resulting particle spins. Moreover, the fibre-like particles examined by Mortensen *et al.* (2008*a*) and Marchioli & Soldati (2013) exhibited reduced spanwise rotation with increasing departure from sphericity.

The directional components of the fluctuating particle angular velocity vector are shown in figure 4. The spin fluctuations are distinctly anisotropic with the highest and lowest levels in the spanwise and streamwise directions respectively. This spin anisotropy reflects the prevailing anisotropy of the vorticity fluctuations in the buffer region. The intensity of the spin fluctuations reduces with the distance from the wall and also tends towards isotropy in the core region.

The spanwise spin fluctuations next to the wall are distinctly larger for $St = 1$ than for $St = 30$. The r.m.s.(ω_y) is furthermore seen to increase with increasing λ beyond $z^+ \approx 15$ to the left in figure 4, but this aspect ratio effect vanishes almost completely for the most inertial particles. This is probably due to the nearly perfect alignment of the $St = 30$ particles in the mean-shear plane.

The spin fluctuations in the wall-normal direction depend on the particle shape in a subtle way. Away from the near-wall region ($z^+ > 15$), r.m.s.(ω_z) increases with λ such that the spheres rotate faster than the flat disks. It should be recalled that the mean spin $\langle\omega_z\rangle = 0$, which implies that the fairly high level of r.m.s.(ω_z) represents a vigorous flipping behaviour superimposed onto the disk-like particle's primary rotation about its almost spanwise-oriented symmetry axis. The fluid viscosity strives to make the particles rotate along with the local vorticity, and the observed particle spin is accordingly a signature of the fluid rotation in the vicinity of the particles. However, the results in figures 3 and 4 show that the flattest particles are partially able to withstand this tendency. This is due to the particle moment of inertia I'_{ij}, which makes the rotational response time of an individual disk-like particle strongly dependent on the aspect ratio. Challabotla *et al.* (2015) showed that the rotational spin-up time for a disk-like particle in uniform shear is

$$\tau_{rotation} = \frac{Da^2}{10\nu}\beta_0, \tag{3.1}$$

where the shape factor β_0 defined in (2.5) is a function of λ. With a fixed relative density D, $\tau_{rotation}$ varies monotonically with the aspect ratio and becomes

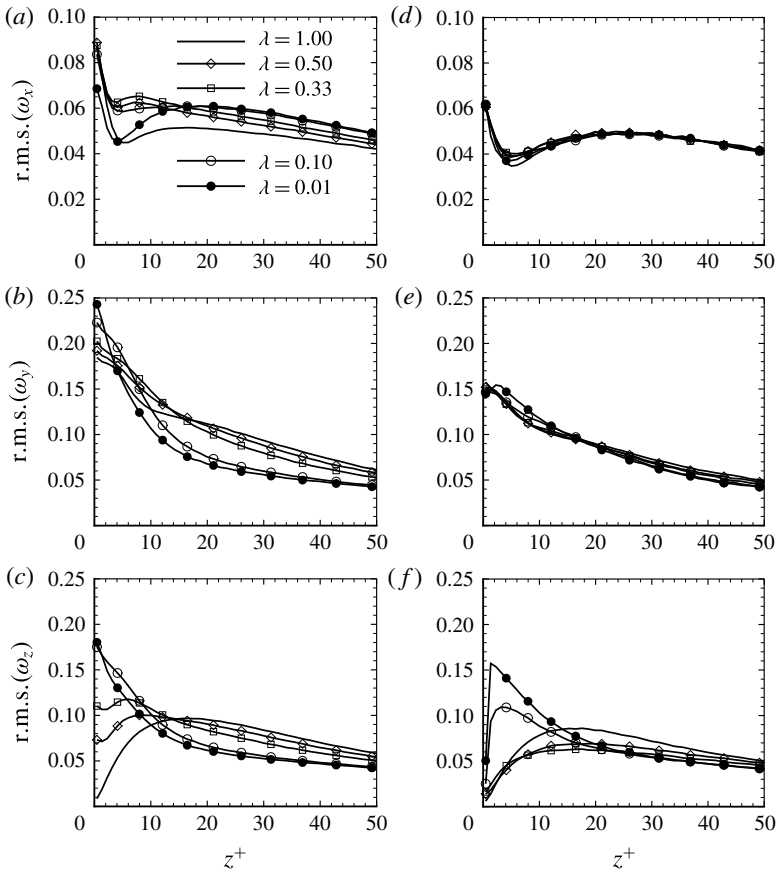

FIGURE 4. Angular velocity fluctuation r.m.s.(ω_i) normalized by the viscous time scale τ_v: (*a–c*) $St = 1$; (*d–f*) $St = 30$.

approximately 40 times longer for a sphere ($\lambda = 1$) than for a disk-like particle with $\lambda = 0.01$. However, in order to maintain the same translational response time τ_p and the same Stokes number St for the differently shaped spheroids, D is about 65 times larger for the $\lambda = 0.01$ particles than for the spheres. The flattest particles considered here have thus a rotational response time $\tau_{rotation}$ about 50 % longer than the spherical particles. The dependence of $\tau_{rotation}$ on the particle shape has a substantial effect on the rotational dynamics in the near-wall region, and the flattest particles are the least amenable to adhering to the local fluid dynamics. However, this influence of λ is substantially reduced at $St = 30$. The latter particles with high translational inertia are fairly resistant to turbulent velocity fluctuations and they are therefore more efficiently spun up by the mean fluid vorticity $\mathrm{d}U/\mathrm{d}z$. They are, on the other hand, less affected by the vorticity fluctuations than the $St = 1$ particles.

4. Concluding remarks

The orientation and rotational dynamics of oblate spheroids suspended in a directly simulated turbulent channel flow have been explored for the first time. We focused on shape effects and considered five different aspect ratios λ in the range from 0.01 to 1, i.e. from rather flattened disk-like particles to spheres. In addition, particles with

both modest and substantial inertia with Stokes numbers St = 1 and 30 respectively were considered. The present study is therefore complementary to earlier DNS studies of fibre-like prolate spheroids by Zhang *et al.* (2001), Mortensen *et al.* (2008*a*,*b*), Marchioli *et al.* (2010) and Marchioli & Soldati (2013) for various aspect ratios $\lambda > 1$.

The translational motion of the oblate spheroids turned out to be weakly dependent on the particle aspect ratio for a given Stokes number. The reason could possibly be that the preferential concentration of the particles in a turbulent flow field is determined mainly by inertia and partly by shape. Shape is, however, crucial for the orientation and rotation of non-spherical particles. For the least inertial spheroids, their orientation as well as their spin showed a strong dependence of the aspect ratio in the near-wall region whereas an isotropization was observed in the channel core irrespective of shape. The inability of the flattest particles ($\lambda \lesssim 0.1$) to achieve a rotation rate comparable to that of the fluid was ascribed to their high rotational inertia which is a combined effect of shape and relative density.

The distinct preferential alignment of the symmetry axis of the inertial oblate spheroids with the mean vorticity vector is qualitatively different from the preferred orientation of prolate spheroids in the streamwise direction. The preferred spanwise orientation resulted in a significant mean spanwise rotation of the disk-like particles. The most inertial particles are more resistant to turbulent velocity fluctuations and the spanwise alignment as well as the spanwise spin increased whereas the influence of shape diminished.

It should be recalled that the viscous drag force F_i from the fluid on a non-spherical particle in (2.2) depends not only on the slip velocity $(u_j - v_j)$, but also on the orientation of the particle in the flow field through the resistance tensor K_{ij} in the inertial frame. Although this paper has been focused on orientation and rotation, the observed preferential particle orientation has a feedback on the drag force and thereby on the particle translational motion.

Acknowledgements

This study has been supported by the Research Council of Norway through research fellowships to N.R.C. and L.Z. (project no 213917/F20, Turbulent Particle Suspensions) and grants of computing time (Programme for Supercomputing).

References

ANDERSSON, H. I. & SOLDATI, A. 2013 Anisotropic particles in turbulence: status and outlook. *Acta Mechanica* **224**, 2219–2223.

BRENNER, H. 1964 The Stokes resistance of an arbitrary particle – IV: arbitrary fields of flow. *Chem. Engng Sci.* **19**, 703–727.

CHALLABOTLA, N. R., NILSEN, C. & ANDERSSON, H. I. 2015 On rotational dynamics of inertial disks in creeping shear flow. *Phys. Lett.* A **379**, 157–162.

DO-QUANG, M., AMBERG, G., BRETHOUWER, G. & JOHANSSON, A. V. 2014 Simulation of finite-size fibers in turbulent channel flows. *Phys. Rev.* E **89**, 013006.

FAN, F. G. & AHMADI, G. 1995 A sublayer model for wall deposition of ellipsoidal particles in turbulent streams. *J. Aero. Sci.* **26**, 813–840.

GALLILY, I. & COHEN, A.-H. 1979 On the orderly nature of the motion of nonspherical aerosol particles. II. Inertial collision between a spherical large droplet and an axially symmetrical elongated particle. *J. Colloid Interface Sci.* **68**, 338–356.

GAUTHIER, G., GONDRET, P. & RABAUD, M. 1998 Motions of anisotropic particles: application to visualization of three-dimensional flows. *Phys. Fluids* **10**, 2147–2154.

GUSTAVSSON, K., EINARSSON, J. & MEHLIG, B. 2014 Tumbling of small axisymmetric particles in random and turbulent flows. *Phys. Rev. Lett.* **112**, 014501.

HARPER, E. Y. & CHANG, I.-D. 1968 Maximum dissipation resulting from lift in a slow viscous shear flow. *J. Fluid Mech.* **33**, 209–225.

JEFFERY, G. B. 1922 The motion of ellipsoidal particles immersed in a viscous fluid. *Proc. R. Soc. Lond.* A **102**, 161–179.

KLEINSTREUER, C. & FENG, Y. 2013 Computational analysis of non-spherical particle transport and deposition in shear flow with application to lung aerosol dynamics – a review. *J. Biomech. Engng* **135**, 021008.

KLETT, J. D. 1995 Orientation model for particles in turbulence. *J. Atmos. Sci.* **52**, 2276–2285.

LUCCI, F., FERRANTE, A. & ELGHOBASHI, S. 2010 Modulation of isotropic turbulence by particles of Taylor length-scale size. *J. Fluid Mech.* **650**, 5–55.

LUNDELL, F. & CARLSSON, A. 2010 Heavy ellipsoids in creeping shear flow: transitions of the particle rotation rate and orbit shape. *Phys. Rev.* E **81**, 016323.

MARCHIOLI, C., SOLDATI, A., KUERTEN, J. G. M., ARCEN, B., TANIÈRE, A., GOLDENSOPH, G., SQUIRES, K. D., CARGNELUTTI, M. F. & PORTELA, L. M. 2008 Statistics of particle dispersion in direct numerical simulations of wall-bounded turbulence: results of an international collaborative benchmark test. *Intl J. Multiphase Flow* **34**, 879–893.

MARCHIOLI, C., FANTONI, M. & SOLDATI, A. 2010 Orientation, distribution, and deposition of elongated, inertial fibers in turbulent channel flow. *Phys. Fluids* **22**, 033301.

MARCHIOLI, C. & SOLDATI, A. 2013 Rotation statistics of fibers in wall shear turbulence. *Acta Mechanica* **224**, 2311–2329.

MARCUS, G. G., PARSA, S., KRAMEL, S., NI, R. & VOTH, G. A. 2014 Measurements of the solid-body rotation of anisotropic particles in 3D turbulence. *New J. Phys.* **16**, 102001.

MORTENSEN, P. H., ANDERSSON, H. I., GILLISSEN, J. J. J. & BOERSMA, B. J. 2008*a* Dynamics of prolate ellipsoidal particles in a turbulent channel flow. *Phys. Fluids* **20**, 093302.

MORTENSEN, P. H., ANDERSSON, H. I., GILLISSEN, J. J. J. & BOERSMA, B.J. 2008*b* On the orientation of ellipsoidal particles in a turbulent shear flow. *Intl J. Multiphase Flow* **34**, 678–683.

NJOBUENWU, D. O. & FAIRWEATHER, M. 2014 Effect of shape on inertial particle dynamics in a channel flow. *Flow Turbul. Combust.* **92**, 83–101.

PARSA, S., CALZAVARINI, E., TOSCHI, F. & VOTH, G. A. 2012 Rotation rate of rods in turbulent fluid flow. *Phys. Rev. Lett.* **109**, 134501.

SHAPIRO, M. & GOLDENBERG, M. 1993 Deposition of glass fiber particles from turbulent air flow in a pipe. *J. Aero. Sci.* **24**, 65–87.

SIEWERT, C., KUNNEN, R. P. J., MEINKE, M. & SCHRÖDER, W. 2014 Orientation statistics and settling velocity of ellipsoids in decaying turbulence. *Atmos. Res.* **142**, 45–56.

UHLMANN, M. 2008 Interface-resolved direct numerical simulation of vertical particulate channel flow in the turbulent regime. *Phys. Fluids* **20**, 053305.

ZHANG, H., AHMADI, G., FAN, F. G. & MCLAUGHLIN, J. B. 2001 Ellipsoidal particles transport and deposition in turbulent channel flows. *Intl J. Multiphase Flow* **27**, 971–1009.

ZHAO, L., MARCHIOLI, C. & ANDERSSON, H. I. 2014 Slip velocity of rigid fibers in turbulent channel flow. *Phys. Fluids* **26**, 063302.